Desalination and Water Treatment
www.deswater.com

doi: 10.5004/dwt.2018.21948

112 (2018) 292–302
April

Sensitivity analysis and modeling of 4-chlorophenol degradation in aqueous solutions by an nZVI-sodium persulfate system

Mansour Baziar[a], Ramin Nabizadeh[a,b,*], Amir Hossein Mahvi[a,c], Kazem Naddafi[a,b], Alireza Mesdaghinia[d], Mahmood Alimohammadi[a,d], Hassan Aslani[e]

[a]*Department of Environmental Health Engineering, School of Public Health, Tehran University of Medical Sciences, Tehran, Iran, Tel. +9821 6695 4234; Fax: +9821 6641 9984; emails: rnabizadeh@tums.ac.ir (R. Nabizadeh), baziar.ehe@gmail.com (M. Baziar), ahmahvi@yahoo.com (A.H. Mahvi), knadafi@tums.ac.ir (K. Naddafi), m_alimohammadi@tums.ac.ir (M. Alimohammadi)*
[b]*Center for Air Pollution Research, Institute for Environmental Research, Tehran University of Medical Sciences, Tehran, Iran*
[c]*Center for Solid Waste Research (CWQR), Institute for Environmental Research (IER), Tehran University of Medical Sciences (TUMS), Tehran, Iran*
[d]*Center for Water Quality Research (CSWR), Institute for Environmental Research (IER), Tehran University of Medical Sciences (TUMS), Tehran, Iran, email: mesdaghinia@tums.ac.ir*
[e]*Health and Environment Research Center, Tabriz University of Medical Sciences, Tabriz, Iran, email: haslani@tbzmed.ac.ir*

Received 12 August 2017; Accepted 24 January 2018

ABSTRACT

In the present study, an artificial neural network (ANN) and response surface methodology (RSM) were used to model the 4-chlorophenol (4-CP) removal in a nanoscale zero-valent iron (nZVI)/persulfate/water system. The impacts of experimental parameters, including persulfate, nZVI, reaction time, pH, and initial 4-CP concentration were considered as input variables in the models. The experiments were conducted based on the central composite design (CCD). The CCD of experiments was also employed as the training set for ANN models. The results of nZVI/persulfate system on removal of 4-CP indicated that the process was directly influenced by the extent of generated sulfate free radicals for the initiation of the oxidative degradation of 4-CP. With increasing the persulfate concentration to 2 mM and nZVI dosage to 1 g/L in the system, the removal percentage of 4-CP was increased. In addition, the acidic condition (pH = 3) turned out to be more favorable than alkaline and neutral conditions for 4-CP elimination. The modeling results showed that ANN with an R^2 value of 0.992 can be more reliable than the RSM model with an R^2 value of 0.9245. A sensitivity analysis was conducted to determine the relative importance of each variable on the ANN model output. The results of the sensitivity analysis showed that all factors were important for model output. However, pH was the most influencing factor.

Keywords: Persulfate; nZVI; ANN; RSM; Sensitivity analysis

1. Introduction

Chlorophenols (CPs) are well-known hazardous, water soluble, toxic, and endocrine-disrupting chemicals which can be discharged into the receiving natural water bodies mainly through industrial wastewater effluents from textile and paint industries, petroleum refining, and solvent, pesticide, and plastic manufacture [1,2]. These compounds are also generated from the chlorination of water containing phenol as well as waste burning [3–5]. They are categorized as toxic pollutants because of their adverse effects on the environment [6,7], cancer- and mutation-causing agents for animal and human beings [1,8], and hardly biodegradable properties [9]. There are various treatment technologies to remove CPs from polluted water and wastewater, such as biological, physicochemical, and advanced oxidation processes (AOPs). However, the high toxicity and bactericidal activities of CPs

* Corresponding author.

and the time-consuming nature of adapting the bacteria which are responsible for treating wastewater containing CPs prevent these kinds of wastewater to be treated by biological treatment methods. Physicochemical processes such as adsorption, air stripping, filtration, flocculation, and precipitation underlie the need for further refinements for lately polluted environment [8]. One of the best strategies for the elimination of CPs and other persistent organic matters is AOPs. The basis of these processes is the generation of powerful reactive species such as hydroxyl ($OH^{\bullet}$) and sulfate free radicals ($SO_4^{-\bullet}$) to partially or entirely mineralize these compounds and/or produce intermediate products with lower toxicity [5,10,11].

In the recent years, the utilization of persulfate (PS) as a common oxidant in aqueous solutions has progressively increased [12]. The interest in utilizing PS for the degradation of recalcitrant organic compounds is related to its redox potential (E^0 = 2.01 V), production of powerful sulfate anion free radical, having a high solubility in aqueous solutions, and its non-selective property and stable structure [12–15].

Although the oxidation potential of PS is relatively high, to increase the efficiency of its overall oxidation potential in water and wastewater remediation, it is activated by heat (Eq. (1)), transition metals (Eq. (2)), and UV light (Eq. (3)) to generate highly reactive sulfate radicals with a higher oxidation potential (E^0 = 2.5–3.1 V) than PS anion [10,16].

$$S_2O_8^{2-} + \text{Heat} \rightarrow 2SO_4^{\bullet -} \quad (1)$$

$$S_2O_8^{2-} + M^{n+} \rightarrow SO_4^{\bullet -} + SO_4^{2-} + M^{(n+1)+} \quad (2)$$

$$S_2O_8^{2-} + h\nu \rightarrow 2SO_4^{\bullet -} \quad (3)$$

In order to generate sulfate free radicals, transition metal ions such as cobalt, silver, and iron are capable of activating the PS through the transfer of one electron. However, silver is expensive and the former creates negative effects on human health. Therefore, their application has been restricted in water and wastewater treatment. The latter is preferred because it is effective, cheap, and not poisonous, and is known as an environmentally friendly activator of PS [9,10,17]. The ferrous ion (Fe^{2+}) may be the best choice among transition metal ions as a PS activator at room temperature. However, it has two main drawbacks. The first drawback is related to its precipitation at pH values equal to or greater than 5 which is the typical pH in water and wastewater remediation. Consequently, the efficiency of remediation systems is reduced due to the quick deactivation of ferrous ions in the systems. The second drawback is originated from the radical-scavenging nature of ferrous ions when their concentrations are high. Hence, a significant number of sulfate free radicals produced at the initial phase of remediation are scavenged by ferrous ions [18].

Recently, nanoscale zero-valent iron (nZVI) has been introduced as an alternative activator of PS gaining popularity among researchers because it is applicable in ambient temperature such as transition metal ions. In addition, its sulfate free radical scavenging in aqueous media is negligible due to the slow release of ferrous ions from nZVI surface [16]. Many researchers have successfully used nZVI as a ferrous ion source for the activation of PS to degrade various pollutants from aqueous solutions, for example, commercial alkyl phenol polyethoxylate [19], bentazon [16], alachlor [20], dichlorodiphenyltrichloroethanes [21], trichloroethylene [22], 2,4-dichlorophenol [23], acetaminophen [12], and bisphenol [24]. Nevertheless, no researcher has yet presented a model for describing the study processes or evaluated the contribution of each parameter in process performance to forecast their future behavior with any change in process parameter values (such as pH and pollutant concentration) which it is likely in the real applications.

Response surface methodology (RSM) is a well-known and efficient statistical approach introduced by Box and Wilson [25]. This approach includes different mathematical, graphical, and statistical techniques which can be used to identify the relationships between process variables and response [25]. Hence, it can be beneficial for improving the performance of treatment processes such as AOPs by apperceiving the feasible interactions among process variables. Although the RSM model can provide good information on the effects of variables and the overall behavior of a system, it may be a complex mathematical model. Compared with this model, intelligent models have been developed by scientists, which can capture experimental data in a proper procedure and provide simple intelligent models.

Artificial neural networks (ANNs) are the most well-known intelligent models introduced along with the expansion of computer and software knowledge [26]. These computational techniques provide three main advantages compared with RSM modeling:

- Capability in modeling a given process without any need for understanding and identification of the complex mechanisms involved in the process.
- No need for a high background of statistic because they are non-parametric models.
- Capability to learn linear and non-linear relationships among variables from a set of examples [27].

Therefore, the main motivations behind the present study were evaluating the performance of nZVI/sodium PS in the elimination of 4-chlorophenol (4-CP) in different operational conditions and developing models with the application of ANN and RSM. The contribution of each operational parameters (sensitivity analysis) in ANN model was also investigated.

2. Materials and methods

2.1. Nanoscale zero-valent iron and chemicals

Sodium persulfate ($Na_2S_2O_8$, ≥99% purity), 4-chlorophenol (4-(Cl)C_6H_4OH, ≥98% purity), 4-aminoantipyrine ($C_{11}H_{13}N_3O$, ≥98% purity), and potassium ferricyanide ($K_3[Fe(CN)_6]$, ≥99% purity) were purchased from Merck Co, Germany. The adjustment of solution pH was performed by H_2SO_4 and NaOH. Other chemicals such as KH_2PO_4, K_2HPO_4, and NH_4OH were analytical grade. nZVI powder with 99.5% purity, 0.45 g/cm^3 density, 8–14 m^2/g surface area, and 35–45 nm particle size was provided from Nanosany Corporation (Iran).

2.2. Experimental procedures

All experiments were carried out in a cylindrical stainless steel reactor with the total volume of 6 L by using 2 L of synthetic water sample at room temperature. During the experiments, in order to avoid any losses of 4-CP from the reactor, it was completely wrapped. For PS activation, the corresponding amount of nZVI powder (0–1 g/L) and sodium persulfate (0–2 mM) was mixed with the proper amount of 4-CP (50–500 mg/L) solution and pH adjustment (3–11) was carried out by 1 M H_2SO_4/NaOH. In order to provide a homogenized mixture of solution in all experiments, the reactor was fixed upon a shaker (model BA-SH300; Pars Tep Company, Iran) throughout predesignated reaction times (5–90 min) of the process. At the end of the reaction time, a certain amount of sample was taken and evaluated to determine the changes in 4-CP concentration. The concentration of 4-CP at different conditions was determined by a UV–visible spectrophotometer at the wavelength of 500 nm (colorimetric method, 5030D, APHA-2005). The removal percentage of 4-CP was calculated based on Eq. (4):

$$\text{Removal}(\%) = \frac{C_i - C_f}{C_i} \times 100 \quad (4)$$

where C_i and C_f are the initial and final concentrations of 4-CP in the process, respectively. It must be noted that, before measuring the 4-CP concentration, the samples were filtrated using 0.22 μm syringe filter to separate the nZVI and diluted with deionized water according to the colorimetric method (5030D, APHA-2005).

2.3. RSM and statistical analysis

RSM is an efficient and empirical statistical modeling tool based on three approaches which are considered to design the experiments' matrix in a study. These approaches are: the expected integrated mean squared error optimal, Box–Behnken design, and central composite design (CCD). The latter is the most frequently approach to design the experiments by RSM [28]. It is able to create models for evaluating the effects of multiple factors and investigating the optimum conditions of variables based on the multiple linear analysis [29]. In the present study, a CCD-based design of experiments with five process parameters, including pH, initial PS concentration, reaction time, initial 4-CP concentration, and initial nZVI dosage was applied. A quadratic model and contour plot responses were constructed. Analysis of variance (ANOVA) which is a set of statistical models was performed using R software to analyze the data and predict the responses [30]. The main role of ANOVA is to understand which variable or which term of the model is statistically significant.

2.4. Artificial neural network modeling

In this study, the Neural Network Toolbox of MATLAB R2013a was employed to forecast the removal percentage of 4-CP from aqueous solutions. In order to develop a predictive model, we constructed a three-layered neural network with one input layer, one hidden layer containing the tangent sigmoid activation function (tansig), and one output layer containing the linear activation function (purelin). The training procedure of the developed models was based on the Levenberg–Marquardt algorithm. This algorithm iteratively updates the input weights (IW), layer weights (LW), and biases (b) of a neural network so that network outputs (predicted values) would be close to the desired values [28,31]. The architecture of the developed neural network and the structure of a neuron in this architecture are shown in Figs. 1 and 2, respectively. As seen in Fig. 1, the number of neurons in the input and output layers was equal to the number of input and output variables, respectively. Therefore, the input layer of the developed AANs had five neurons corresponding to the process parameters: pH, initial PS concentration, reaction time, initial 4-CP concentration, and initial nZVI dosage. Also, the output layer had one neuron corresponding to the removal percentage of 4-CP. However, for network structure optimization, it is very important to determine the hidden layer neurons.

In order to guarantee a constant approach and limit the computational trouble throughout the training process, ANN model inputs and outputs were normalized between –1 and 1.

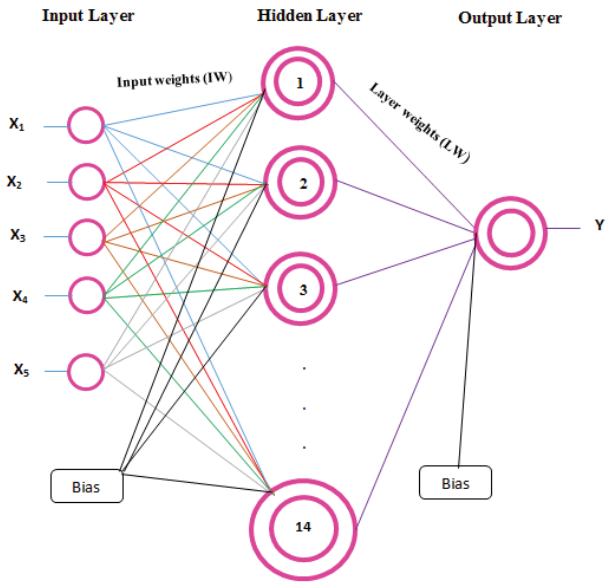

Fig. 1. The architecture of the developed neural network (5-14-1).

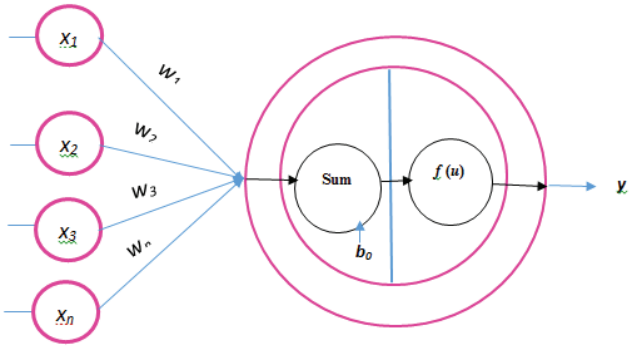

Fig. 2. Structure of a neuron in the best developed ANN model, $f(u)$ in hidden and output layers equals tansig and purelin, respectively.

Moreover, the data were randomly divided into three subsets (80% for training, 10% for validation, and 10% for testing) to evaluate the robustness of the developed models. MATLAB normalization was done by Eq. (5):

$$y = \frac{x_i - x_{\min}}{x_{\max} - x_{\min}} \times (b - a) + a \tag{5}$$

where y is normalized value x_i, $x_{\max}$, and $x_{\min}$ are the maximum and minimum values of experimental data, respectively; and a and b equal to –1 and 1, respectively. The performance of the developed ANN models was handled based on the indices of mean squared error (MSE) and correlation coefficient (R).

3. Results and discussion

3.1. Central composite design and fitting quadratic model

According to the CCD, a set of 62 experiments, comprising 32 factorial points, 10 axial points, and 20 center points at two blocks was obtained by the R software 3.3.2. The levels and range of each variable are given in Table 1. In order to calculate the coded values of the considered variables, Eq. (6) was applied:

$$x_i = \frac{X_i - X_j}{\delta X} \tag{6}$$

Here, x_i denotes the coded value, δX represents the step change, and X_i and X_j, respectively, are the real value of operating parameter (independent variable) and real value of operating parameter in the center point [32].

A total set of experimental runs and corresponding responses of 4-CP elimination are presented in Table 2. A second-order polynomial equation (Eq. (7)), which can describe linear, quadratic, and interactions terms of variables was fitted to the experimental results to assess the mathematical relationship between the five operating factors and 4-CP removal percentage.

$$y = \beta_0 + \sum_{i=1}^{5} \beta_i x_i + \sum_{i=1}^{5} \sum_{j=1}^{5} \beta_{ij} x_i x_j + \sum_{i=1}^{5} \beta_{ii} x_i^2 + \varepsilon \tag{7}$$

Table 1
Experimental parameters and coded levels of variables

Factor	Variable	Coded levels				
		–1	–0.42	0	0.42	1
pH	X_1	3	5.3	7	8.7	11
Persulfate (mM)	X_2	0	0.58	1	1.42	2
Reaction time (min)	X_3	5	30	47.5	65	90
4-CP (mg/L)	X_4	50	180	275	369	500
nZVI dosage (g/L)	X_5	0	0.3	0.5	0.7	1

In which y (response) indicates the predicted removal (%); x_i and x_j denote operating parameters (independent factors); and β_0 shows the coefficient of model intercept. Parameters of β_i, β_{ii}, and β_{ij} are the coefficients for linear, quadratic, and cross-product (interaction) terms, respectively [33]. To validate the adequacy of the developed quadratic model, ANOVA was applied. The coefficient of determination (R^2) and adjusted coefficient of determination along with model lack of fit were also calculated to figure out the goodness of the model. Table 3 presents the results of ANOVA on the experimental data by applying the multiple regression analysis. A quadratic regression equation (Eq. (8)) was generated from the analysis which included five main effects (linear terms), three quadratic effects (quadratic terms), and seven interaction effects (interaction terms), in which Y is 4-CP elimination, and X_1, X_2, X_3, X_4, and X_5 are pH, initial PS concentration, reaction time, initial 4-CP concentration, and initial nZVI dosage, respectively. The p values of each term were evaluated to determine their significance.

$$\begin{aligned} Y = {} & 43.926 - 7.664X_1 + 9.866X_2 + 3.917X_3 - 3.833X_4 \\ & + 7.95X_5 - 7.009X_1X_2 + 4.576X_1X_4 - 15.71X_1X_5 \\ & - 11.718X_2X_3 - 8.038X_2X_4 - 10.237X_3X_5 \\ & - 5.764X_4X_5 + 14.763X_1^2 + 10.818X_3^2 - 7.196X_5^2 \end{aligned} \tag{8}$$

The results of the developed quadratic model (Table 3) indicated that the effects of X_1, X_2, X_3, X_4, X_5 (linear terms), X_1X_2, X_1X_5, X_2X_3, X_2X_4, X_3X_5, X_4X_5 (interaction terms), and X_1^2, X_3^2 and X_5^2 (quadratic terms) were significant ($p < 0.05$). The fit of the quadratic model was evaluated with R^2, adjusted R^2, and lack-of-fit index. In the present study, the values of R^2, adjusted R^2, and model lack of fit equaled 0.9245, 0.8877, and 0.05069, respectively. Furthermore, p value and F statistic of the model were 2.2×10^{-16} and 32.19, respectively. Thus, it can be concluded that the pattern of 4-CP removal is properly explained by the model.

3.2. Effect of zero-valent iron nanoparticles' dose

Zero-valent iron nanoparticles are a potential source of Fe^{2+}. They have an ability to provide ferrous iron ions from the surface as well as supply the needed Fe^{2+} ions permanently without any radical scavenger feature. In the sodium persulfate/nZVI system, PS is converted to sulfate radicals through supplied ferrous iron ions during the surface oxidation of nZVI [12,17,18,36]. These generated sulfate radicals can decompose 4-CP. In addition, in aqueous solutions, the oxidation of nZVI via dissolved oxygen can also generate superoxide radicals and reactive oxygen species (hydroxyl and Fe(IV)) which can improve system performance (Fig. 3) [34]. In this study, we measured the DO level only at the beginning of the process which was about 2 mg/L.

To determine the effects of nZVI dose on the elimination of 4-CP, various amounts of nZVI (0, 0.3, 0.5, 0.7, and 1 g/L) were employed. The TEM and SEM pictures of the used nZVI along with the certificate of analysis are presented in Fig. 4. The contour plots of nZVI vs. pH, nZVI vs. reaction time, and nZVI vs. initial 4-CP concentration are presented in Figs. 5(a)–(c), respectively. As can be seen in these contour

Table 2
Central composite design of experiments and responses for 4-CP removal

Runs	Variables					Response Removal	Runs	Variables					Response Removal
	X_1	X_2	X_3	X_4	X_5			X_1	X_2	X_3	X_4	X_5	
1	8.7	0.58	30	180	0.29	34.8	32	7	1	47.5	275	0.5	46
2	5.3	1.42	30	180	0.29	50.8	33	7	1	47.5	275	0.5	43.6
3	8.7	0.58	30	369	0.29	39	34	5.3	0.58	65	180	0.71	56.12
4	8.7	1.42	65	180	0.29	48.32	35	8.7	1.42	65	369	0.29	46.11
5	5.3	0.58	30	180	0.71	52	36	7	1	47.5	275	0.5	43.41
6	5.3	1.42	30	180	0.71	67	37	5.3	1.42	65	180	0.29	57.23
7	5.3	1.42	30	369	0.71	60.4	38	8.7	0.58	65	369	0.29	49.95
8	8.7	0.58	65	180	0.29	46.7	39	5.3	1.42	65	180	0.71	66.94
9	8.7	1.42	30	180	0.71	56.5	40	8.7	0.58	30	369	0.71	39.23
10	7	1	47.5	275	0.5	46.41	41	8.7	1.42	65	369	0.71	40.14
11	5.3	0.58	30	180	0.29	35	42	7	1	47.5	275	0.5	42.31
12	5.3	1.42	65	369	0.29	48.93	43	11	1	47.5	275	0.5	47.41
13	8.7	1.42	30	369	0.71	51.4	44	7	1	47.5	500	0.5	39.34
14	8.7	1.42	65	180	0.71	50.23	45	3	1	47.5	275	0.5	63.8
15	8.7	0.58	30	180	0.71	37.65	46	7	1	47.5	275	0.5	45.41
16	5.3	1.42	30	369	0.29	45.94	47	7	1	47.5	275	0	24.52
17	7	1	47.5	275	0.5	45.41	48	7	1	47.5	275	1	42.77
18	8.7	1.42	30	180	0.29	47.12	49	7	1	47.5	275	0.5	40.26
19	7	1	47.5	275	0.5	43.54	50	7	0	47.5	275	0.5	27.5
20	7	1	47.5	275	0.5	43.21	51	7	1	47.5	275	0.5	46.34
21	7	1	47.5	275	0.5	44.1	52	7	1	47.5	275	0.5	44.32
22	8.7	0.58	65	180	0.71	45.23	53	7	1	47.5	50	0.5	46.34
23	7	1	47.5	275	0.5	46	54	7	1	47.5	275	0.5	45.36
24	8.7	1.42	30	369	0.29	44.6	55	7	1	47.5	275	0.5	43.12
25	5.3	0.58	65	369	0.71	49.6	56	7	2	47.5	275	0.5	47.35
26	5.3	0.58	30	369	0.71	48.23	57	7	1	47.5	275	0.5	39.96
27	5.3	0.58	30	369	0.29	35.5	58	7	1	5	275	0.5	47
28	8.7	0.58	65	369	0.71	42.48	59	7	1	47.5	275	0.5	39.54
29	5.3	0.58	65	369	0.29	44.36	60	7	1	47.5	275	0.5	42.7
30	5.3	1.42	65	369	0.71	57.3	61	7	1	90	275	0.5	56.32
31	5.3	0.58	65	180	0.29	44.7	62	7	1	47.5	275	0.5	44.76

plots, the removal percentage of 4-CP increases with increasing the nZVI dosage. The best nZVI dosage to achieve maximum removal efficiency was found to be 1 g/L. In fact, the highest elimination of 4-CP was attained at maximum concentration of ferrous ions due to the higher generation of sulfate free radicals with increasing the nZVI dosage. Two hypotheses are possible for ferrous ion production in the ZVI–peroxydisulfate (PDS) system. The first is that, during the Fenton-like reaction, electron is transferred directly from ZVI to PDS by a mechanism similar to Haber–Weiss. The second is that both aerobic and anaerobic conditions might have caused iron corrosion via the following reaction:

$$2Fe^0 + O_2 + 2H_2O \rightarrow 2Fe^{2+} + 4OH^- \quad (9)$$

$$Fe^0 + 2H_2O \rightarrow Fe^{2+} + 2OH^- + H_2 \quad (10)$$

Iron can possibly induce reductive PDS decomposition as it is a strong electron donor. Furthermore, PDS per se is

Table 3
Estimated coefficients of the fitted quadratic model on 4-CP removal percentage

Model term	Coefficient estimate	SE	*t* Value	*p* Value
Intercept	43.926	0.508	88.448	2.20×10^{-16}
X_1	–7.664	0.951	–8.058	2.42×10^{-10}
X_2	9.866	0.951	10.374	1.24×10^{-13}
X_3	3.917	0.951	4.118	1.56×10^{-4}
X_4	–3.833	0.951	–4.031	2.06×10^{-4}
X_5	7.950	0.951	8.362	8.75×10^{-11}
X_1:X_2	–7.009	2.631	–2.663	0.010
X_1:X_4	4.576	2.631	1.739	0.088
X_1:X_5	–15.710	2.631	–5.969	3.215×10^{-7}
X_2:X_3	–11.718	2.631	–4.452	5.36×10^{-5}
X_2:X_4	–8.038	2.631	–3.0544	0.003
X_3:X_5	–10.237	2.631	–3.890	0.0003
X_4:X_5	–5.764	2.631	–2.190	0.033
X_1^2	14.763	1.837	7.938	3.64×10^{-10}
X_3^2	10.818	1.837	5.791	5.94×10^{-7}
X_5^2	–7.196	1.837	–4.013	0.0002

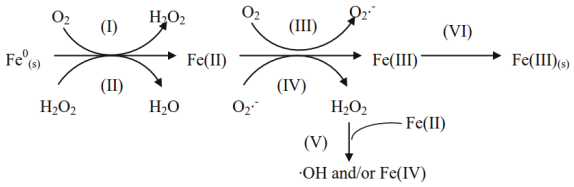

Fig. 3. Generation of superoxide radicals and reactive oxygen species from nZVI.

an oxidant, tending to snitch electron to produce sulfate radical, the presence of which improves the dissolution of ZVI (Eq. (11)), the same as aqueous oxygen [17].

$$S_2O_8^{2-} + Fe^0 \rightarrow 2SO_4^{2-} + Fe^{2+} \quad (11)$$

3.3. Effect of persulfate and 4-CP concentration on 4-CP elimination

The results of nZVI/PS system on the removal of 4-CP imply that the process was directly influenced by the extent of generated sulfate free radicals to the initiation of the oxidative degradation of 4-CP. With increasing the PS concentration from 0 to 2 mM, removal efficiency was increased. This behavior may be explained by the increase in the amount of generated sulfate free radicals. The highest removal was observed in higher concentrations of PS (2 mM). The contour plots of PS vs. pH, PS vs. reaction time, and PS vs. initial 4-CP concentration are presented in Figs. 5(d)–(f), respectively. The removal efficiency also depended on the initial amounts of 4-CP concentration (Fig. 5(f)). The influence of initial concentration on 4-CP elimination in the nZVI/PS system was examined in the range of 50–500 mg/L. Based on the contour plot of PS vs. initial 4-CP concentration, the removal percentage increases with increasing the PS concentration and decreasing 4-CP concentration. This can be due to the lower covering of active sites for PS on the iron surface [14]. In higher concentrations of 4-CP, its molecules can be adsorbed on the nZVI surface and can reduce active sites on the iron surface for PS activation. Therefore, free reactive radicals are not formed enough in the nZVI/PS system to break down the 4-CP [17].

3.4. Effect of reaction time and pH on 4-CP elimination

Figs. 5(b) and (e) show that changes in 4-CP concentration are a function of reaction time. Based on these figures, removal efficiency increases with increasing the nZVI dosage

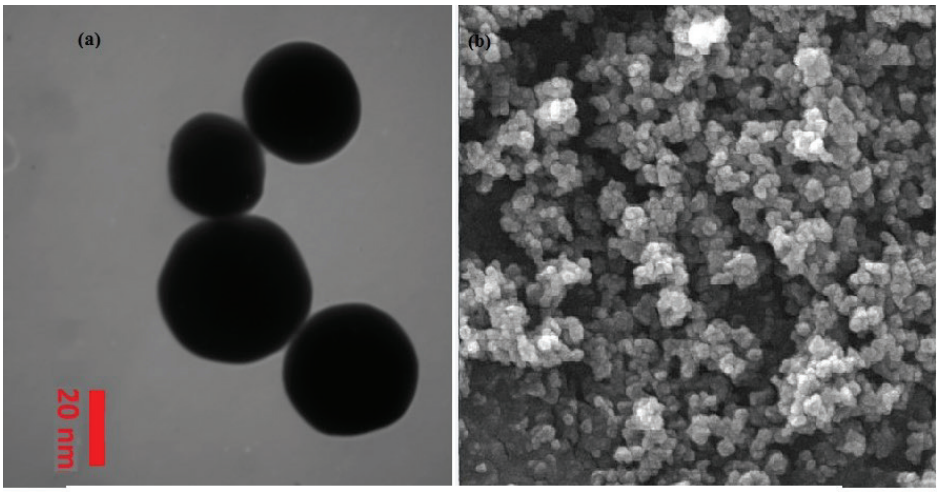

Certificate of Analysis-%											
Fe	Cu	Si	Ni	Cr	Mg	Al	Ti	Mo	Pb	Mn	Ca
≥99.5	≤0.005	≤0.02	≤0.12	≤0.015	≤0.004	≤0.091	≤ 0.005	≤0.024	≤0.004	≤0.13	≤0.044

Fig. 4. Characterization of nZVI: (a) TEM and (b) SEM.

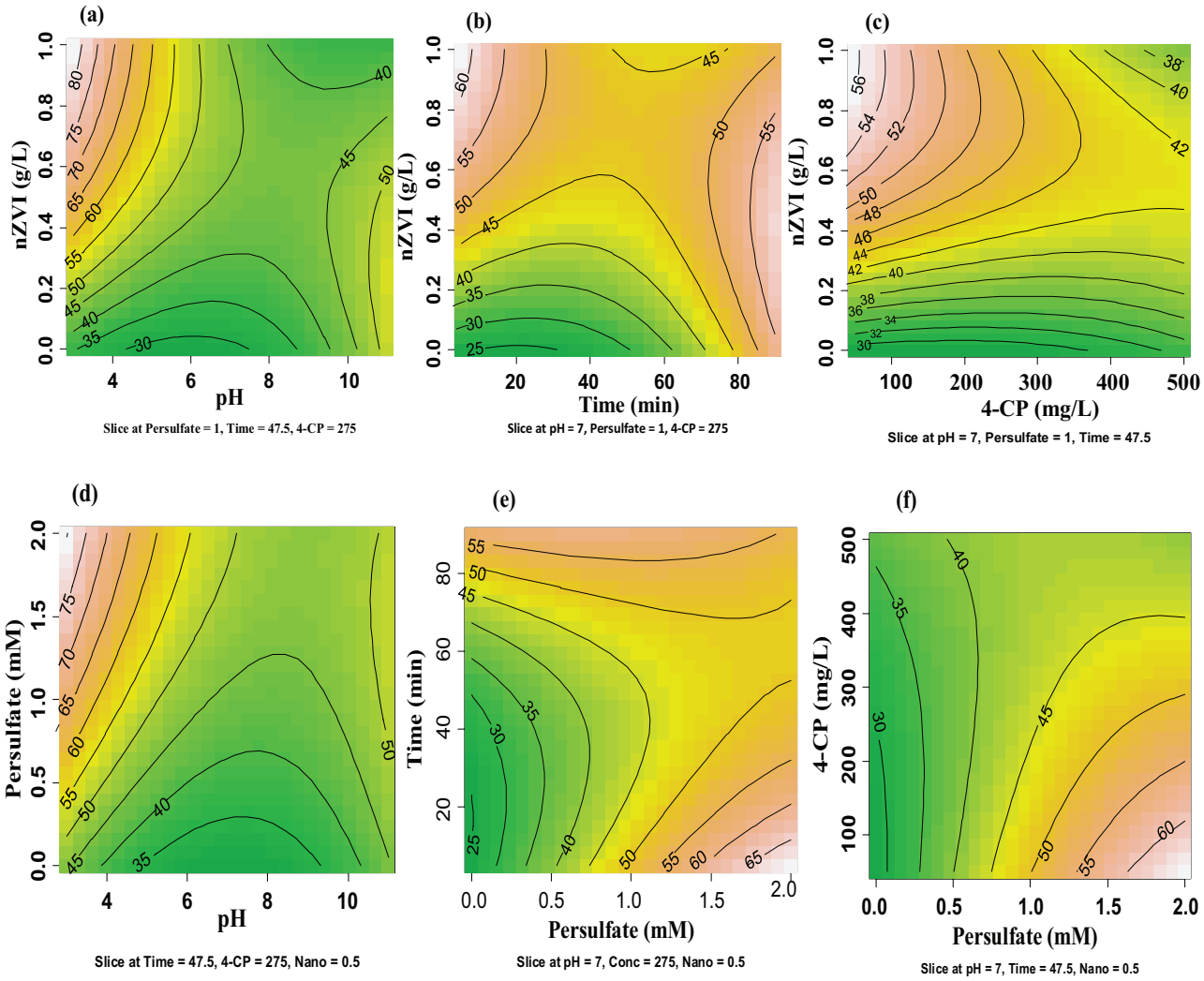

Fig. 5. Contour plots of 4-CP elimination in the nZVI/persulfate system as a function of (a) pH and nZVI dose; (b) time and nZVI dose; (c) 4-CP concentration and nZVI dose; (d) pH and persulfate; (e) persulfate and time; (f) persulfate and 4-CP concentration.

and PS concentration increasing along with the reaction time. This can be due to the fact that nZVI is a source of ferrous iron and can release ferrous iron gradually to generate sulfate free radicals [12].

Figs. 5(a) and (d) demonstrate the effect of pH in the nZVI/PS system. Based on these figures, the removal efficiency increases with decreasing solution pH and increasing nZVI and PS concentrations. It is demonstrated that the acidic condition is more favorable than alkaline and neutral conditions for the removal of 4-CP. This may be because the more the increase in H^+ concentration, and consequently the more the acid catalyzation, the greater the $SO_4^{-\bullet}$ formation [12]. Since this is known as one of the most important oxidants, rise of this active species can lead to further degradation of 4-CP. It is believed that the PS oxidation process which involves $SO_4^{-\bullet}$ or $^{\bullet}OH$ has an important contribution to the fractionation of organic contaminants in PS–ZVI systems. Accordingly, in order to identify the existence of $SO_4^{-\bullet}$ and $^{\bullet}OH$, radical scavenger tests are utilized during pollutant breakdown in the PS/Fe^0 process. It has been shown by Zhao et al. [17] that methanol addition as $SO_4^{-\bullet}$ and $^{\bullet}OH$ scavengers completely quenches the reaction in the PS–ZVI system, which could be moderately repressed through adding TBA as an $^{\bullet}OH$ scavenger. They further recommended that $SO_4^{-\bullet}$ be the principal radical species capable of degrading 4-CP. Hussain et al. [13] reported similar results on scavenger tests. Also, previous reports indicate that acidic conditions favored sulfate radical predominance whereas hydroxyl radical was more conspicuous in basic conditions [35]. Additionally, the corrosion of Fe^0 might have been exacerbated by the initial acidic pH, leading to further release of Fe^{2+} and possible PS activation. The formation of SO_4 increases in acidic conditions because of acid-catalyzation through Eqs. (12) and (13) [36].

$$S_2O_8^{2-} + H^+ \rightarrow HS_2O_8^- \quad (12)$$

$$HS_2O_8^- \rightarrow SO_4^{\bullet -} + SO_4^{2-} + H^+ \quad (13)$$

As also pointed out by Bremner et al. [37] and Kusic et al. [38], $SO_4^{-\bullet}$ formation from PS is hastened by acidic pH levels during ZVI/PS oxidation.

Removal percentage is low in alkaline and neutral pHs. This can be due to the precipitation of ferrous and ferric ions (Fe^{3+} and Fe^{2+}) and the formation of (oxy)hydroxides. Whereas these (oxy)hydroxides are insoluble in higher pH, they have little ability to produce sulfate free radicals in terms of activating the PS. Additionally, another plausible justification can be attributed to the fact that alkaline and neutral pH increase the occurrence of passivation on the surface of nZVI. The following equations are proposed for the formation of (oxy)hydroxides in the system [13,14].

$$Fe^{3+} + H_2O \rightarrow FeOH^{2+} + H^+ \quad (14)$$

$$Fe^{3+} + 2H_2O \rightarrow Fe2\left(OH_2\right)^{4+} + 2H^+ \quad (15)$$

$$2Fe^{3+} + 2H_2O \rightarrow Fe2\left(OH\right)_2^{4+} + 2H^+ \quad (16)$$

$$Fe^{2+} + 2OH^- \rightarrow Fe(OH)_2 \quad (17)$$

Nevertheless, in higher alkaline conditions of the nZVI/PS system, 4-CP can be removed due to the alkaline activation of PS and generation of sulfate radicals. The alkaline activation of PS can be explained with Eq. (18) [14]:

$$2S_2O_8^{2-} + 2H_2O \rightarrow SO_4^{\bullet -} + 3SO_4^{2-} + O_2^{-\bullet} + 4H^+ \quad (18)$$

Zhao et al. [17] suggested a mechanism for the degradation of 4-CP in which 4-CP is charged by free radicals to remove chlorine (Cl) atoms from the structure of compound, leading to the production of hydroquinone. The molecules of this compound are then converted into 1,4-benzoquinone in the dehydrogenation process. The degradation of 1,4-benzoquinone ring is facilitated by the presence of excess free radicals in the system, resulting in the formation of aliphatic acids which eventually produce CO_2 molecules in a series of successive oxidation steps.

3.5. Reusability

A critical feature of a catalyst is its constancy for environmental technology applications. Thus, this research examined the efficiency of catalyst recycle through a two-cycle trial for 4-CP fractionation conducted separately under similar settings. To do this, initial concentrations of 4-CP (180 mg/L), nZVI (0.71 g/L), and PS (1.42 mM) were used in pH = 5.3 and the reaction time of 30 min. The residual solution from the breakdown of the catalyst was filtered and rinsed and the solid was dried by following each experiment. Under identical experimental conditions, the dried catalyst samples were reused for 4-CP degradation. After two catalytic cycles, a decrease in catalytic activity from 67% to 55% of degraded 4-CP was obtained by recycling trials. Such reduced catalytic activity may have been caused by partial deactivation of the catalyst surface resulting from continuous adsorption of intermediate species [39].

3.6. ANN-based modeling

To design a robust ANN-based model, various hidden layer neurons from 1 to 30 were investigated. The maximum value of correlation coefficient (R) and the minimum value of MSE for training, validation, and testing sets were employed to choose the best ANN model architecture. The results of different neuron numbers and corresponding R and MSE values are presented in Table 4. It was found that, when the network developed with a total hidden-layer neurons equals to 14 (bold values) resulted to the R values 0.998, 0.985, and 0.999 and corresponding MSE values 0.0003, 0.004, and 0.003 for training, validation, and testing sets, respectively. Thus, the suitable structure of the developed ANN-based model (Fig. 1) was one input layer with five neurons (pH, initial PS concentration, reaction time, initial 4-CP concentration, and initial nZVI dosage), one hidden layer with 14 neurons, and one output layer with one neuron (percentage removal). Fig. 6(a) illustrates the predicted values of 4-CP removal in training, validation, testing, and all prediction sets vs. experimental result data. This figure also includes the best linear fit, namely $y = 1.0096x - 0.3459$ and $R^2 = 0.9926$ for all datasets. The R^2 value of 0.9926 demonstrates that the developed model with 5-14-1 structure can explain 99.26% of variation in the forecasted and actual values. The distribution of residual errors (actual value–forecasted value) for training, validation, and test datasets is shown in Fig. 6(b). As seen in this figure, the deviancy of residual error values was relatively low. These results illustrate that there is good compatibility between ANN forecasted values and experimental values.

3.7. Sensitivity analysis

To determine the relative importance of each variable (input variables) on model output, a sensitivity analysis based on the neural network weight matrix (an equation method proposed by Garson for the best ANN model) was carried out. The principal of the Garson equation (Eq. (19)) is partitioning ANN connection weights [40]. Table 5 displays the weight matrix produced for the ANN model in this study.

$$I_j = \frac{\sum_{m=1}^{m=N_h}\left(\left(\frac{\left|W_{jm}^{ih}\right|}{\sum_{k=1}^{N_i}\left|W_{km}^{ih}\right|}\right)\times\left|W_{mm}^{ho}\right|\right)}{\sum_{k=1}^{k=N_i}\left\{\sum_{m=1}^{m=N_h}\left(\left(\frac{\left|W_{km}^{ih}\right|}{\sum_{k=1}^{N_i}\left|W_{km}^{ih}\right|}\right)\times\left|W_{mm}^{ho}\right|\right)\right\}}\times 100 \quad (19)$$

Here, I_j is the relative importance (%) of the jth parameter on the ANN model output; N_h and N_i are hidden and input layer neurons, respectively; W is related to ANN connection weights; o, h, and i indices belong to output, hidden, and input layers, respectively; and n, m, and k are neuron numbers in output, hidden, and input layers, respectively [40].

Table 4
Dependence among the number of neurons in the hidden layer, *R* value, and MSE, for ANN models with normalized data

Neuron number	Training		Validation		Testing	
	MSE	*R* value	MSE	*R* value	MSE	*R* value
1	0.077	0.742	0.107	0.694	0.21	0.385
2	0.042	0.815	0.036	0.805	0.148	0.705
3	0.051	0.798	0.031	0.805	0.029	0.847
4	0.003	0.99	0.029	0.806	0.035	0.703
5	0.008	0.968	0.004	0.951	0.06	0.906
6	0.0007	0.997	0.01	0.98	0.0008	0.96
7	0.002	0.99	0.016	0.968	0.034	0.979
8	0.0005	0.997	0.009	0.911	0.036	0.921
9	0.0009	0.995	0.026	0.954	0.019	0.976
10	0.0002	0.999	0.089	0.943	0.007	0.986
12	0.0004	0.998	0.051	0.974	0.09	0.899
13	0.002	0.993	0.033	0.971	0.002	0.983
14	**0.0003**	**0.998**	**0.004**	**0.985**	**0.003**	**0.999**
15	0.0003	0.998	0.013	0.982	0.017	0.961
16	0.0007	0.997	0.0137	0.944	0.023	0.968
17	0.021	0.943	0.011	0.982	0.027	0.979
18	0.00027	0.999	0.0024	0.987	0.024	0.94
19	0.0019	0.989	0.093	0.914	0.0242	0.963
20	0.00027	0.998	0.032	0.906	0.039	0.959
21	0.0009	0.996	0.003	0.995	0.088	0.937
22	0.015	0.964	0.089	0.952	0.022	0.963
23	0.012	0.963	0.021	0.911	0.081	0.84
24	0.0026	0.992	0.03	0.974	0.096	0.969
25	0.0003	0.998	0.028	0.948	0.071	0.847
26	0.0088	0.974	0.033	0.941	0.03	0.933
27	0.035	0.927	0.117	0.818	0.175	0.786
28	0.003	0.992	0.052	0.926	0.292	0.791
29	0.0004	0.997	0.093	0.908	0.135	0.729
30	0.001	0.994	0.03	0.934	0.06	0.904

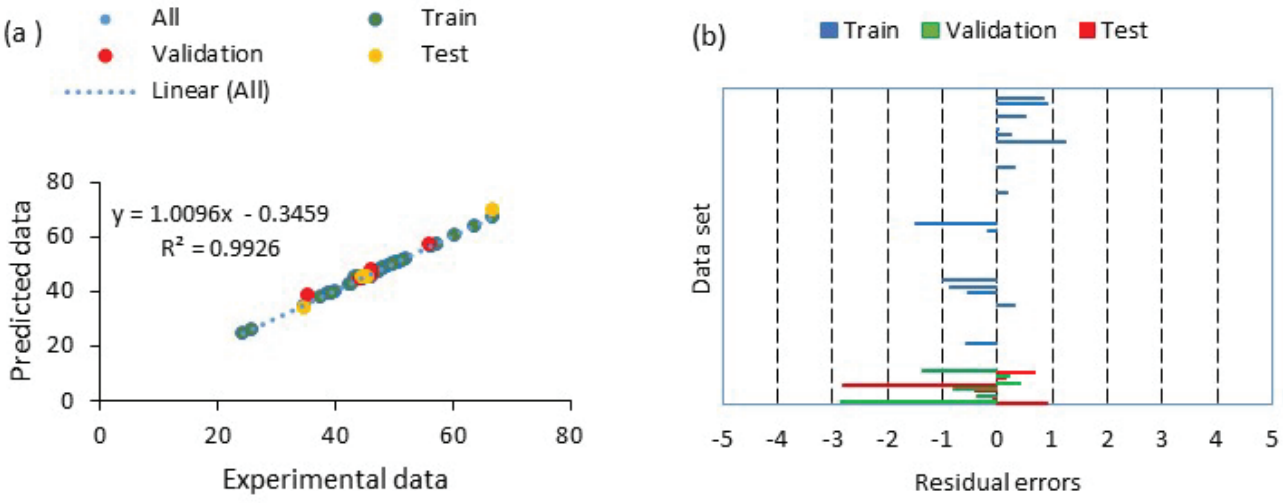

Fig. 6. Comparison of ANN results and experimental data (a); distribution of the residual for training, validation, and test dataset (b).

Table 5
Weight and bias of the best ANN model for predicting 4-CP removal percentage

IW					LW^T	b_1	b_2
1.518628	–1.04586	1.413719	0.287241	–1.2686	0.482159	–2.48118	1.299198
–0.4296	1.26927	0.185531	–2.04892	–1.18118	0.220419	–2.17489	
1.555476	–1.65967	0.258721	0.685857	0.554752	–0.16221	–1.39814	
–3.11045	–0.11676	0.21455	–0.0115	0.805976	–0.5466	1.423577	
1.529564	1.130762	1.811308	0.000547	–0.20865	0.317926	–0.02818	
0.609527	–0.24904	–2.97201	0.124271	0.393033	0.412573	–1.40354	
–1.18197	0.998874	0.864887	0.432602	1.344101	0.527666	0.802924	
1.375719	–0.52982	–0.13855	0.241853	0.874112	–0.51392	–0.40302	
–1.3547	1.722667	–0.36756	–0.77425	–0.30471	0.787023	–0.94785	
0.533585	–1.11101	–0.72458	–1.29487	0.92901	0.157115	0.774891	
–0.27671	1.269644	–0.34452	–0.85994	–1.52719	–0.76521	–0.86711	
–0.17664	–2.04424	–0.60571	–0.5584	–0.4185	0.475402	1.502436	
–0.55601	–1.20138	1.475061	–0.39737	1.045335	0.502038	–2.25196	
1.368722	–0.65426	–0.7786	–0.77425	–1.3465	–0.47125	2.625223	

It is clear that all input variables (pH, PS concentration, reaction time, initial 4-CP concentration, and nZVI dosage) had potential effects on 4-CP removal. However, the most important variable was pH with a relative importance of 26%, followed by PS concentration, nZVI dosage, and reaction time with an importance of 24%, 20%, and 18%, respectively. Furthermore, the least relative importance belonged to 4-CP concentration (with an importance of 12%). These indicate that the selected range of nZVI and PS is reliable for a variety strength of synthetic wastewater.

4. Conclusion

We studied a process of oxidation which employed nZVI in combination with sodium persulfate. The process was successful in the removal of 4-CP by producing free radicals such as sulfate. The present study showed that the combination of nZVI and sodium persulfate can be a possible strategy for the removal of organic matters from aqueous solutions. In the modeling step, the effects of various operating parameters, including nZVI dosage, reaction time, PS concentration, pH, and 4-CP concentration on removal percentage were assessed by applying ANN and RSM techniques. The forecasted removal percentage, achieved from ANN and RSM, was compared with experimental removal in terms of determination coefficient (R^2) value. The ANN method with the R^2 value of 0.992 was superior to the RSM model in catching the linear and non-linear pattern of the nZVI/PS system. To determine the relative importance of each variable (input variables) on model output, a sensitivity analysis based on the neural network weight matrix was used for the best ANN model. The results showed that all input variables (pH, PS concentration, reaction time, initial 4-CP concentration, and nZVI dosage) have potential effects on 4-CP removal. Nevertheless, the most important variable is pH, followed by PS concentration, nZVI dosage, reaction time, and 4-CP concentration.

Acknowledgments

This study was funded by a grant (Project No.: 95-01-46-31639) from the Center for Water Quality Research (CWQR), Institute for Environmental Research (IER), Tehran University of Medical Sciences (TUMS), Tehran, Iran, as Mansour Baziar's PhD dissertation. The authors would like to express their gratitude to the Department of Environmental Health Engineering, School of Public Health, Tehran University of Medical Sciences for their cooperation.

References

[1] S.S. Shinde, C.H. Bhosale, K.Y. Rajpure, Photocatalytic oxidation of salicylic acid and 4-chlorophenol in aqueous solutions mediated by modified $AlFe_2O_3$ catalyst under sunlight, J. Mol. Catal. A: Chem., 347 (2011) 65–72.
[2] B. Deka, K.G. Bhattacharyya, Using coal fly ash as a support for Mn(II), Co(II) and Ni(II) and utilizing the materials as novel oxidation catalysts for 4-chlorophenol mineralization, J. Environ. Manage., 150 (2015) 479–488.
[3] U.G. Ahlborg, T.M. Thunberg, H.C. Spencer, Chlorinated phenols: occurrence, toxicity, metabolism, and environmental impact, Crit. Rev. Toxicol., 7(1980) 1–35.
[4] X. Liu, J.H. Fan, L.M. Ma, Elimination of 4-chlorophenol in aqueous solution by the bimetallic Al–Fe/O_2 at normal temperature and pressure, Chem. Eng. J., 236 (2014) 274–284.
[5] M.D. Marković, B.P. Dojčinović, B.M. Obradović, J. Nešić, M.M. Natić, T.B. Tosti, M.M. Kuraica, D.D. Manojlović, Degradation and detoxification of the 4-chlorophenol by non-thermal plasma-influence of homogeneous catalysts, Sep. Purif. Technol., 154 (2015) 246–254.
[6] Z. Ai, P. Yang, X. Lu, Degradation of 4-chlorophenol by a microwave assisted photocatalysis method, J. Hazard. Mater., 124 (2005) 147–152.

[7] P. Yan, L. Xu, J. Xia, Y. Huang, J. Qiu, Q. Xu, Q. Zhang, H. Li, Photoelectrochemical sensing of 4-chlorophenol based on Au/BiOCl nanocomposites, Talanta, 156 (2016) 257–264.
[8] M. Pera-Titus, V. García-Molina, M.A. Baños, J. Giménez, S. Esplugas, Degradation of chlorophenols by means of advanced oxidation processes: a general review, Appl. Catal., B, 47 (2004) 219–256.
[9] F.-x. Ye, D.-s. Shen, Acclimation of anaerobic sludge degrading chlorophenols and the biodegradation kinetics during acclimation period, Chemosphere, 54 (2004) 1573–1580.
[10] L.W. Matzek, K.E. Carter, Activated persulfate for organic chemical degradation: a review, Chemosphere, 151 (2016) 178–188.
[11] C.B. Molina, J.A. Zazo, J.A. Casas, J.J. Rodriguez, CWPO of 4-CP and industrial wastewater with Al–Fe pillared clays, Water Sci. Technol., 61 (2010) 2161–2168.
[12] J. Deng, Y. Shao, N. Gao, Y. Deng, C. Tan, S. Zhou, Zero-valent iron/persulfate (Fe^0/PS) oxidation acetaminophen in water, Int. J. Environ. Sci. Technol., 11 (2014) 881–890.
[13] I. Hussain, Y. Zhang, S. Huang, X. Du, Degradation of *p*-chloroaniline by persulfate activated with zero-valent iron, Chem. Eng. J., 203 (2012) 269–276.
[14] I. Hussain, Y. Zhang, S. Huang, Degradation of aniline with zero-valent iron as an activator of persulfate in aqueous solution, RSC Adv., 4 (2014) 3502–3511.
[15] J. Yan, L. Han, W. Gao, S. Xue, M. Chen, Biochar supported nanoscale zerovalent iron composite used as persulfate activator for removing trichloroethylene, Bioresour. Technol., 175 (2015) 269–274.
[16] X. Wei, N. Gao, C. Li, Y. Deng, S. Zhou, L. Li, Zero-valent iron (ZVI) activation of persulfate (PS) for oxidation of bentazon in water, Chem. Eng. J., 285 (2016) 660–670.
[17] J. Zhao, Y. Zhang, X. Quan, S. Chen, Enhanced oxidation of 4-chlorophenol using sulfate radicals generated from zero-valent iron and peroxydisulfate at ambient temperature, Sep. Purif. Technol., 71 (2010) 302–307.
[18] M.A. Al-Shamsi, N.R. Thomson, Treatment of organic compounds by activated persulfate using nanoscale zerovalent iron, Ind. Eng. Chem. Res., 52 (2013) 13564–13571.
[19] K. Temiz, T. Olmez-Hanci, I. Arslan-Alaton, Zero-valent iron-activated persulfate oxidation of a commercial alkyl phenol polyethoxylate, Environ. Technol., 37 (2016) 1757–1767.
[20] Q. Wang, Y. Shao, N. Gao, W. Chu, J. Deng, X. Shen, X. Lu, Y. Zhu, X. Wei, Degradation of alachlor with zero-valent iron activating persulfate oxidation, J. Taiwan Inst. Chem. Eng., 63 (2016) 379–385.
[21] C. Zhu, G. Fang, D.D. Dionysiou, C. Liu, J. Gao, W. Qin, D. Zhou, Efficient transformation of DDTs with persulfate activation by zero-valent iron nanoparticles: a mechanistic study, J. Hazard. Mater., 316 (2016) 232–241.
[22] Y.T. Lin, C. Liang, C.W. Yu, Trichloroethylene degradation by various forms of iron activated persulfate oxidation with or without the assistance of ascorbic acid, Ind. Eng. Chem. Res., 55 (2016) 2302–2308.
[23] X. Li, M. Zhou, Y. Pan, L. Xu, Pre-magnetized Fe^0/persulfate for notably enhanced degradation and dechlorination of 2,4-dichlorophenol, Chem. Eng. J., 307 (2017) 1092–1104.
[24] L. Zhao, Y. Ji, D. Kong, J. Lu, Q. Zhou, X. Yin, Simultaneous removal of bisphenol A and phosphate in zero-valent iron activated persulfate oxidation process, Chem. Eng. J., 303 (2016) 458–466.
[25] M.A. Bezerra, R.E. Santelli, E.P. Oliveira, L.S. Villar, L.A. Escaleira, Response surface methodology (RSM) as a tool for optimization in analytical chemistry, Talanta, 76 (2008) 965–977.
[26] M. Afrand, M.H. Esfe, E. Abedini, H. Teimouri, Predicting the effects of magnesium oxide nanoparticles and temperature on the thermal conductivity of water using artificial neural network and experimental data, Physica E, 87 (2017) 242–247.
[27] J.P. Maran, V. Sivakumar, K. Thirugnanasambandham, R. Sridhar, Artificial neural network and response surface methodology modeling in mass transfer parameters predictions during osmotic dehydration of *Carica papaya* L., Alexandria Eng. J., 52 (2013) 507–516.
[28] S. Chamoli, ANN and RSM approach for modeling and optimization of designing parameters for a V down perforated baffle roughened rectangular channel, Alexandria Eng. J., 54 (2015) 429–446.
[29] J.P. Maran, B. Priya, Comparison of response surface methodology and artificial neural network approach towards efficient ultrasound-assisted biodiesel production from muskmelon oil, Ultrason. Sonochem., 23 (2015) 192–200.
[30] R.V. Lenth, Response-surface methods in R using RSM, J. Stat. Software, 32 (2009) 1–17.
[31] M.T. Hagan, M.B. Menhaj, Training feedforward networks with the Marquardt algorithm, IEEE Trans. Neural Networks, 5 (1994) 989–993.
[32] M. Shams, M.H. Dehghani, R. Nabizadeh, A. Mesdaghinia, M. Alimohammadi, A.A. Najafpoor, Adsorption of phosphorus from aqueous solution by cubic zeolitic imidazolate framework-8: modeling, mechanical agitation versus sonication, J. Mol. Liq., 224 (2016) 151–157.
[33] M.H. Muhamad, S.R. Abdullah, A.B. Mohamad, R.A. Rahman, A.A. Kadhum, Application of response surface methodology (RSM) for optimisation of COD, NH_3–N and 2,4-DCP removal from recycled paper wastewater in a pilot-scale granular activated carbon sequencing batch biofilm reactor (GAC-SBBR), J. Environ. Manage., 121 (2013) 179–190.
[34] J. Fan, H. Wang, L. Ma, Oxalate-assisted oxidative degradation of 4-chlorophenol in a bimetallic, zero-valent iron–aluminum/air/water system, Environ. Sci. Pollut. Res., 23 (2016) 16686–16698.
[35] C. Liang, Z.S. Wang, C.J. Bruell, Influence of pH on persulfate oxidation of TCE at ambient temperatures, Chemosphere, 66 (2007) 106–113.
[36] J. Li, Q. Liu, Q. Ji, B. Lai, Degradation of *p*-nitrophenol (PNP) in aqueous solution by Fe^0-PM-PS system through response surface methodology (RSM), Appl. Catal., B, 200 (2017) 633–646.
[37] D.H. Bremner, A.E. Burgess, D. Houllemare, K.-C. Namkung, Phenol degradation by using hydroxyl radicals generated from zero-valence iron and hydrogen peroxide, Appl. Catal., B, 63 (2006) 15–19.
[38] H. Kusic, I. Peternel, N. Koprivanac, A. Loncaric Bozic, Iron activated persulfate oxidation of an azo dye in model wastewater: influence of iron activator type on process optimization, J. Environ. Eng., 137 (2011) 454–463.
[39] A.E. Pirbazari, M.A. Zanjanchi, Heterogeneous photocatalytic degradation of 4-chlorophenol by immobilization of cobalt tetrasulphophthalocyanine onto MCM-41, Korean J. Chem. Eng., 31 (2014) 218–223.
[40] E.S. Elmolla, M. Chaudhuri, M.M. Eltoukhy, The use of artificial neural network (ANN) for modeling of COD removal from antibiotic aqueous solution by the Fenton process, J. Hazard. Mater., 179 (2010) 127–134.